Screening of Elasticity by Plastic Charges in Amorphous Solids

Itamar Procaccia

The Weizmann Institute of Science

Rehovot 76100 Israel

Work with M. Moshe, H. Charan, Y. Jin, A. Kumar, A. Lemaitre, C. Mondal, B. Bhowmik, S. Roy, T. Samanta, J. Shang, J. Zhang

Kyoto August 2023

Examples of glassy materials

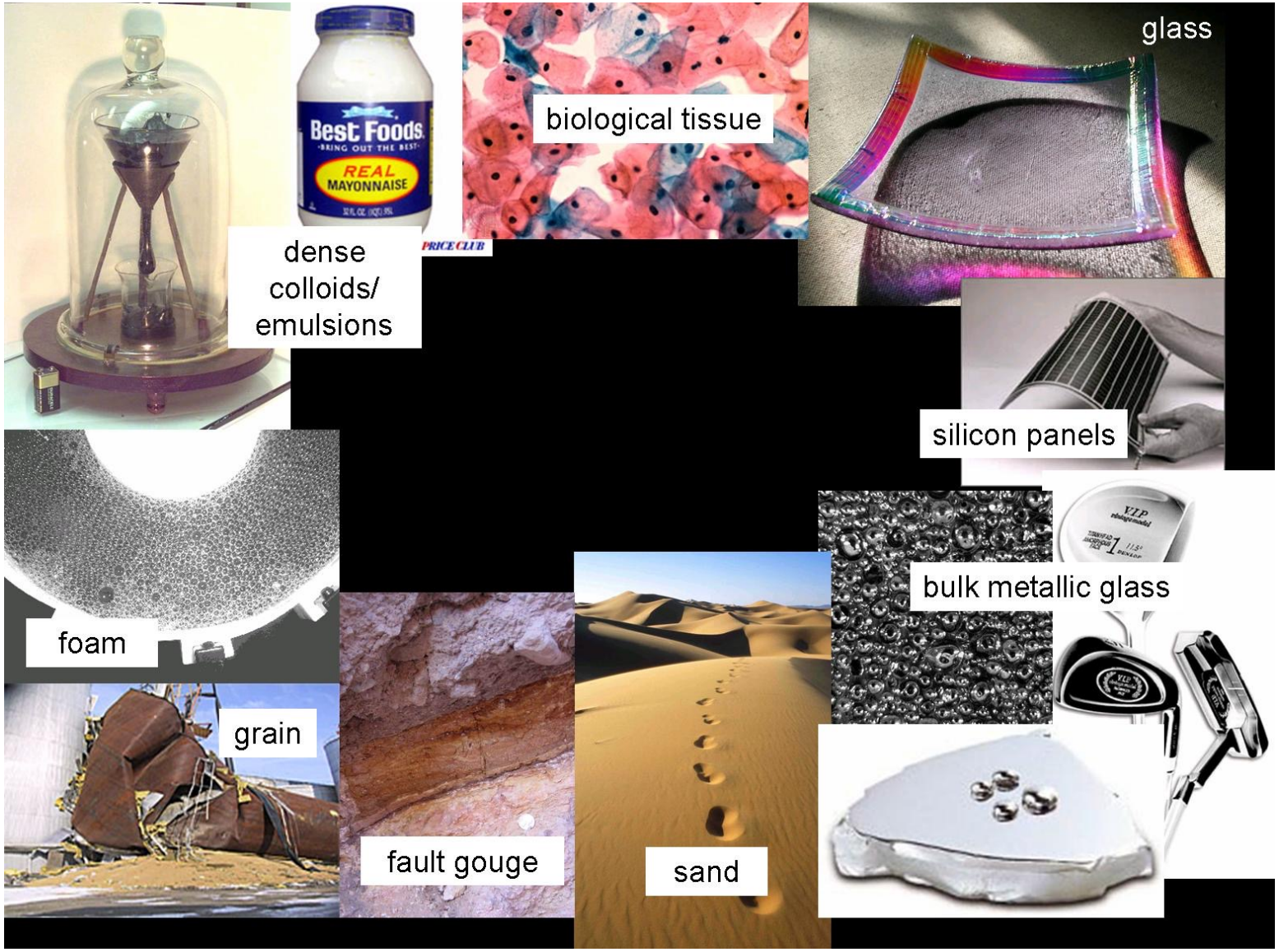

In a paper that was uploaded to the Arxive recently

I. INTRODUCTION

From the point of view of elasticity, a glass is a very simple solid, elastically isotropic, described by a density ρ, a bulk modulus B and a shear modulus G. Consequently, one has isotropic longitudinal and transverse sound velocities v_l and v_t, respectively.

- In fact we know that (in the thermodynamic limit) plasticity sets in immediately, for any amount of strain. Phys. Rev. E. 82,055103 (2010)
- Typically plastic events exhibit quadrupolar symmetry (Eshelby).
- Plasticity has profound effect. Upshot of this talk:
- Small amounts of plasticity: classical elasticity remains valid but the elastic moduli get dressed. Screening by quadrupoles.
- High amounts of plasticity: elasticty theory is modified. Screening by dipoles.
- The analogy to Kosterlitz-Thouless and Hexatic transitions

Respecting the constraints of time, I will consider a very simple setup, of an amorphous solids confined to an annulus of radii $r_{\rm in}$ and $r_{\rm out}$, $r_{\rm in} \ll r_{\rm out}$

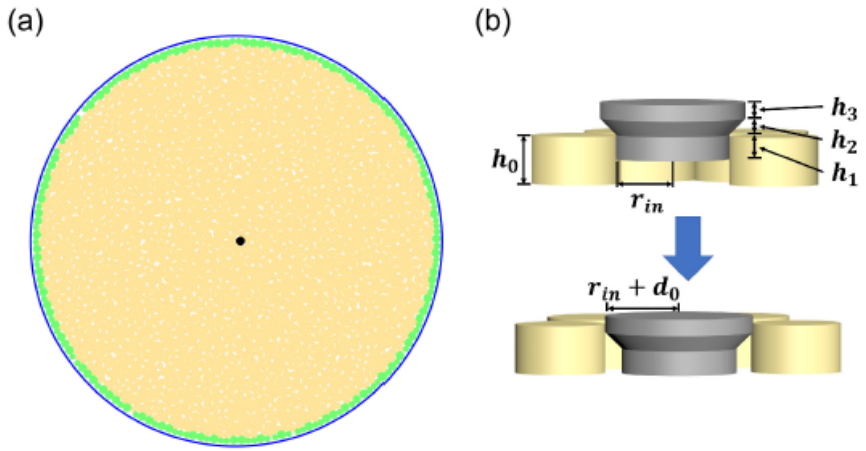

FIG. 1. Panel (a): Top view of the experimental system. The blue line marks the position of the circular boundary. The green layer represent the photo-elastic disks at the circumference, which are used as pressure sensors. In the yellow area, either the bi-disperse ABS disks or the bi-disperse photo-elastic disks are filled in, see text for details. The black dot in the center represents the conical shaped pusher used to achieve the inflation. Panel (b) A diagram of the inflation process. Here $r_{in} = 7.0$ mm, $d_0 = 0.7$ mm, $h1 = 2.0$ mm, $h2 = 0.7$ mm, and $h_3 = 3.0$ mm for the conical shaped pusher in the low dimensionless pressure experiment, and $r_{in} = 14.0$ mm, $d_0 = 1.4$ mm, $h1 = 2.0$ mm, $h2 = 1.4$ mm, and $h_3 = 3.0$ mm in the high dimensionless pressure experiment. The value of h_0 depends on the pusher type: $h_0 = 8.0$ mm for the ABS disks, and $h_0 = 6.0$ mm for the photo-elastic disks.

We then impose a displacement

$$\mathbf{d}(r_{\rm in}) = d_0\hat{r} \text{ and } \mathbf{d}(r_{\rm out}) = 0.$$

What is the resulting displacement field?

Let us consult classical elasticity theory

$$F = \int \mathcal{L}\,\mathrm{d}^2x - \oint t^\beta d_\beta\,\mathrm{d}l\ ,$$

$$\mathcal{L} = \frac{1}{2}A^{\alpha\beta\gamma\delta}u_{\alpha\beta}u_{\gamma\delta} = \frac{1}{2}\sigma^{\alpha\beta}u_{\alpha\beta}\ .$$

$$u_{\alpha\beta} = \frac{1}{2}\left(\partial_\alpha d_\beta + \partial_\beta d_\alpha\right)\ .$$

$$\delta_d F = \delta_d \int \mathcal{L} \mathrm{d}^2 x - \oint t^\beta \delta d_\beta \mathrm{d}l$$
$$= \int \mathrm{d}^2 x \sigma^{\alpha\beta} \delta u_{\alpha\beta} - \oint t^\beta \delta d_\beta \mathrm{d}l \ .$$

$$\partial_\alpha \sigma^{\alpha\beta} = 0$$
$$\sigma^{\alpha\beta} n_\beta|_\partial = t^\alpha \ .$$

In this radial geometry $\mathrm{d}(r) = d_r(r)\hat{r}$ and classical elasticity dictates

$$d_r'' + \frac{d_r'}{r} - \frac{d_r}{r^2} = 0$$

$$d_r(r) = d_0 \frac{r^2 - r_{\mathrm{out}}^2}{r_{\mathrm{in}}^2 - r_{\mathrm{out}}^2} \frac{r_{\mathrm{in}}}{r} \ .$$

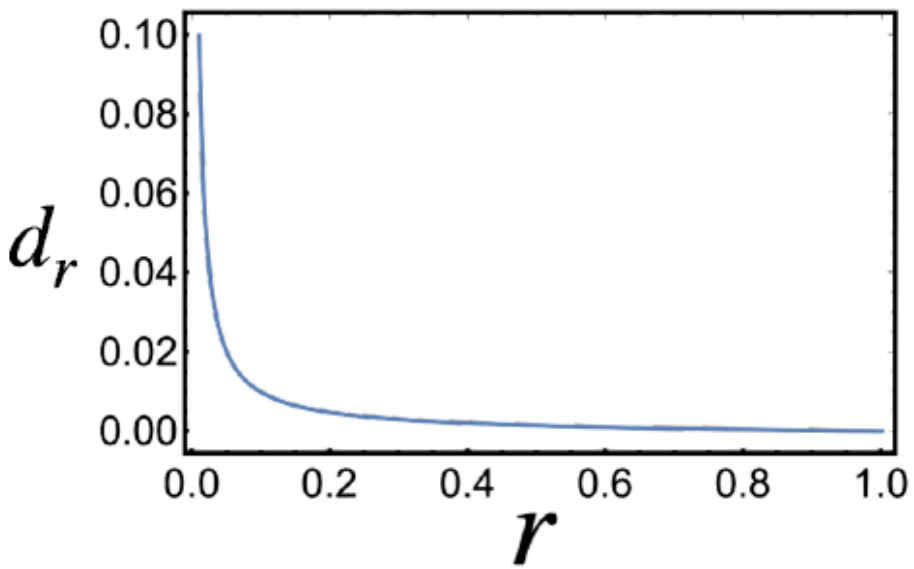

Examples of measured displacement fields in classical glass formers

Sometimes…

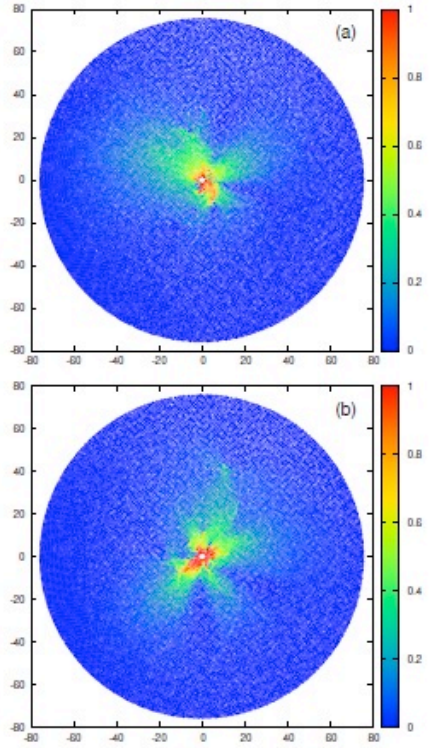

FIG. 1. Examples of quasi-elastic responses associated with inflation of the inner disk at $r_{\rm in}$. These examples correspond with panels (a) and (b) of Fig. 3. he parameters associated with these examples are $T_m = 0.4$ and 0.3 respectively, $d_0 = 0.15$ and 0.18, $r_{\rm in} = 0.72$ and 0.8, and $r_{\rm out} = 76$ for both.

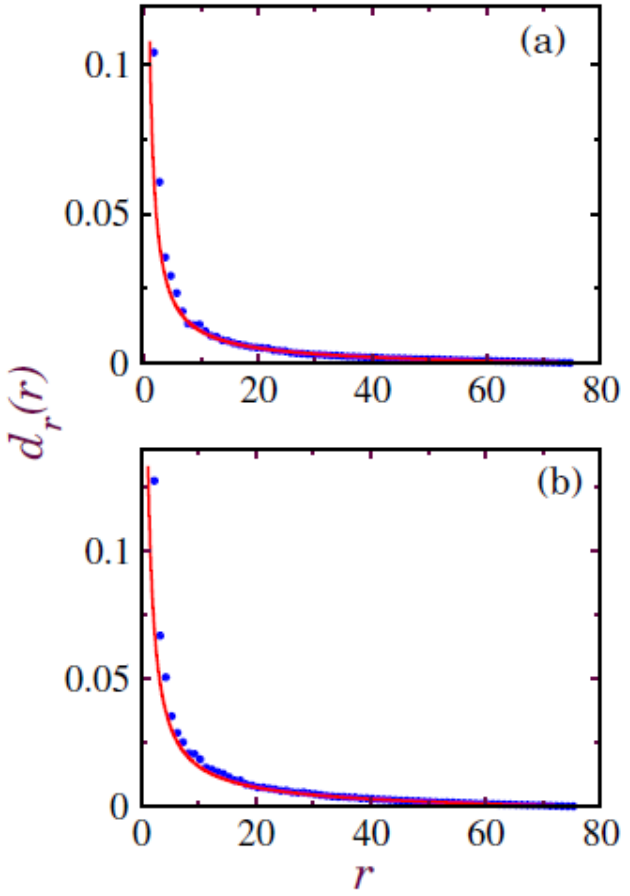

FIG. 3. Typical quasi-elastic angle-averaged displacement field.

And sometimes…

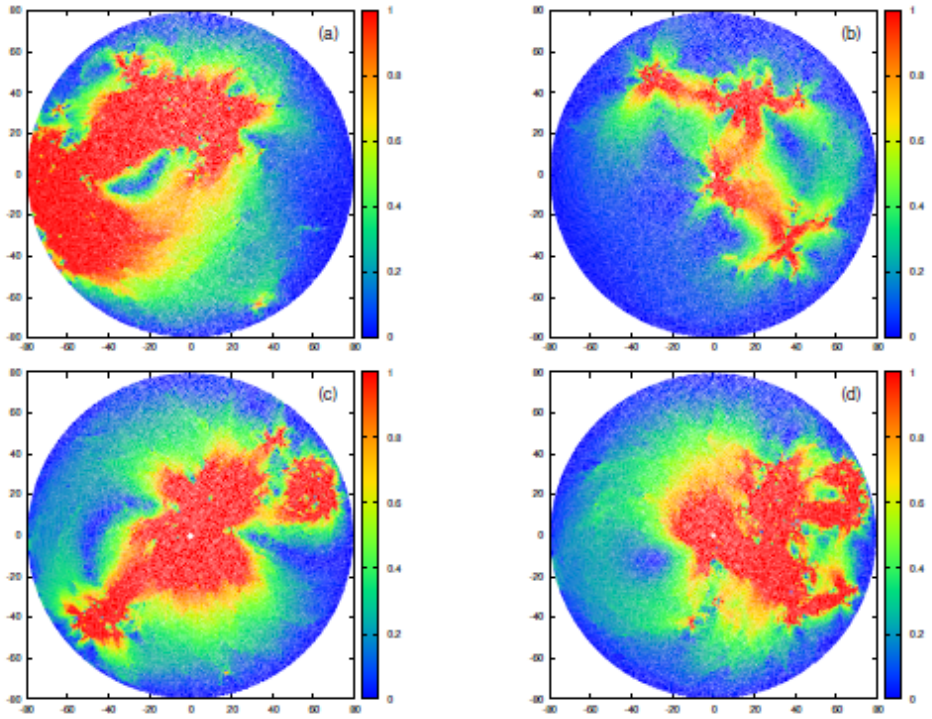

FIG. 2. Examples of "anomalous" displacement fields associated with an inflation of the inner disk at $r_{\rm in}$. The examples shown here correspond to panels (a)-(d) in Fig. 4.

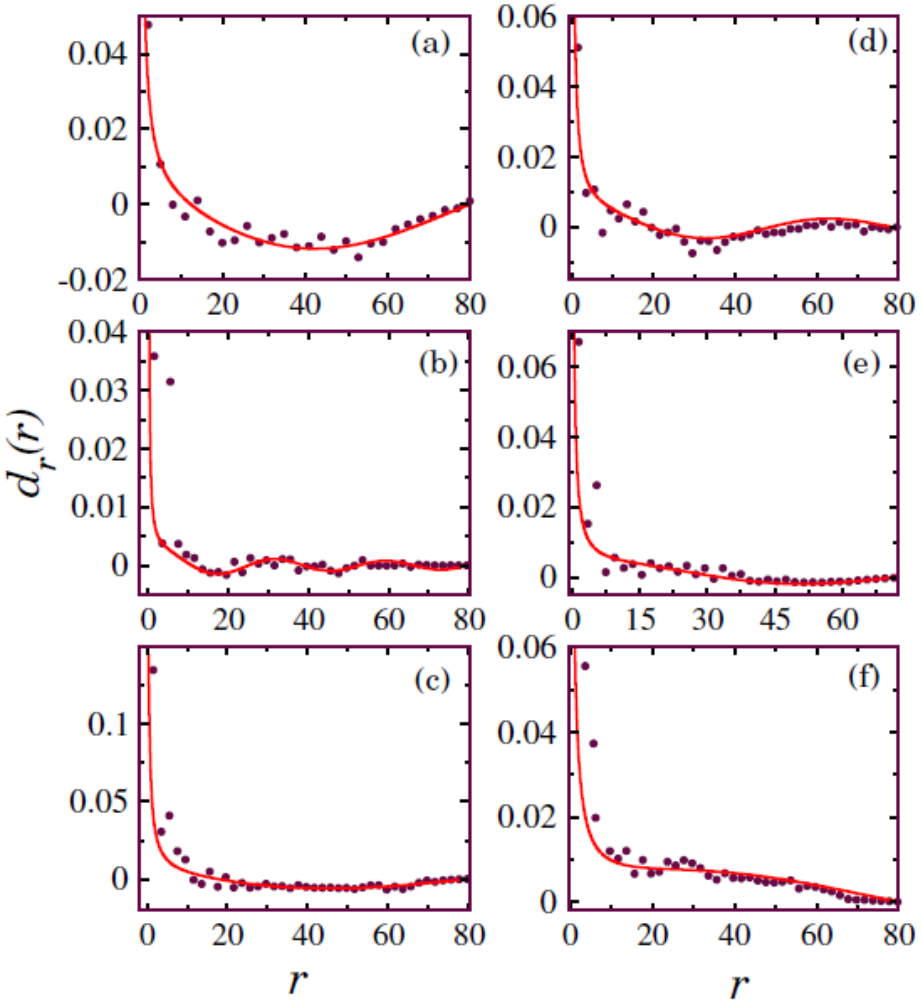

FIG. 4. Typical anomalous angle-averaged displacement fields. The parameters of the simulation and the value of the "anmoaly parameter" κ are presented in table I.

The effect of dilute quadrupoles Phy. Rev. E. 104, 024904 2021.

Written symbolically

$$U = U_{\text{el}} + U_{\text{QQ}} + U_{\text{Q-el}}$$

R. Dasgupta, H. G. E. Hentschel, and I. Procaccia, Microscopic mechanism of shear bands in amorphous solids, Phys. Rev. Lett. **109**, 255502 (2012).

$$U_{\text{el}} = \int \mathrm{d}^2x \frac{1}{2} A^{\alpha\beta\gamma\delta} u_{\alpha\beta} u_{\gamma\delta}$$

$$U_{\text{QQ}} = \int \mathrm{d}^2x \frac{1}{2} \Lambda_{\alpha\beta\gamma\delta} Q^{\alpha\beta} Q^{\gamma\delta}$$

$$U_{\text{Q-el}} = \int \mathrm{d}^2x \Gamma^{\alpha\beta}_{\gamma\delta} u_{\alpha\beta} Q^{\gamma\delta} \ .$$

Upon minimization of the energy we obtain the same equations as before but with renormalized elastic moduli.

This is the situation analogous to dielectrics!

The effect of large density of quadrupoles

The new ingredient: we cannot neglect gradients of the quadrupole density $\hat{P}^\alpha \equiv \partial_\beta Q^{\alpha\beta}$,

In the presence of dipoles, the most general isotropic and homogeneous quadratic energy is

$$\mathcal{L} = \frac{1}{2} A^{\mu\nu\rho\sigma} u_{\mu\nu} u_{\rho\sigma} + \frac{1}{2} \Lambda_{\alpha\beta} P^\alpha P^\beta + \Gamma^\alpha{}_\beta d_\alpha P^\beta \ .$$

Upon minimizing the energy $\Delta \mathbf{d} + \left(1 + \frac{\lambda_1}{\lambda_2}\right) \nabla (\nabla \cdot \mathbf{d}) = -\frac{\mu_1^2}{\mu_2 \lambda_2} \mathbf{d}$

Broken translational symmetry!!

In polar coordinates

$$d_r'' + \frac{1}{r} d_r' + (\kappa^2 - \frac{1}{r^2}) d_r = 0 \ .$$

$$d_r(r) = d_0 \frac{Y_1(r\,\kappa) J_1(r_{\rm out}\kappa) - J_1(r\,\kappa) Y_1(r_{\rm out}\kappa)}{Y_1(r_{\rm in}\kappa) J_1(r_{\rm out}\kappa) - J_1(r_{\rm in}\kappa) Y_1(r_{\rm out}\kappa)}$$

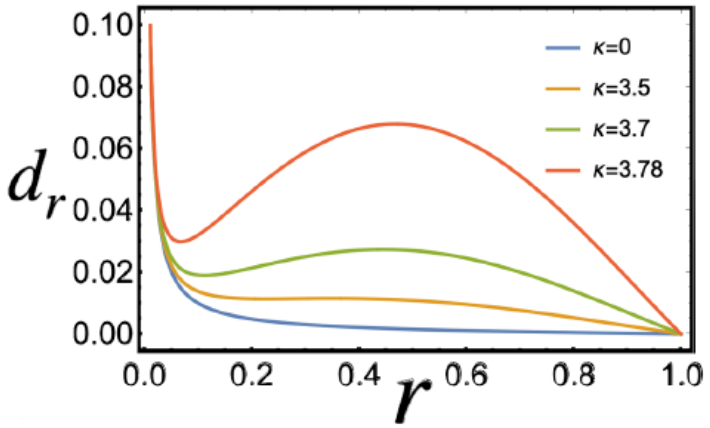

FIG. 6. The solutions of Eq. (45) for different values of the parameter κ. Here $r_{\rm in} = 0.01$ and $r_{\rm out} = 1$, with $d_r(r_{\rm in}) = 0.1$ and $d_r(r_{\rm out}) = 0$.

Three dimensions?

K-T transition and Hexatic do not exist in 3-dimensions

Our theory (if correct) extends smoothly to 3-dimensions

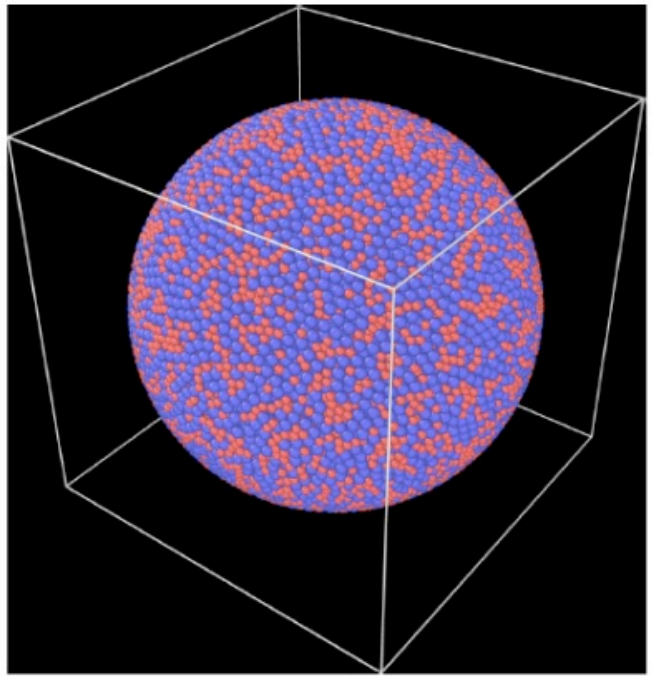

FIG. 2. Typical configuration of our system of $N = 42876$ bi-dispersed little spheres with volume fraction $\phi = 0.647$.

Inflate a small sphere in the center, equilibrated and measure the displacement field

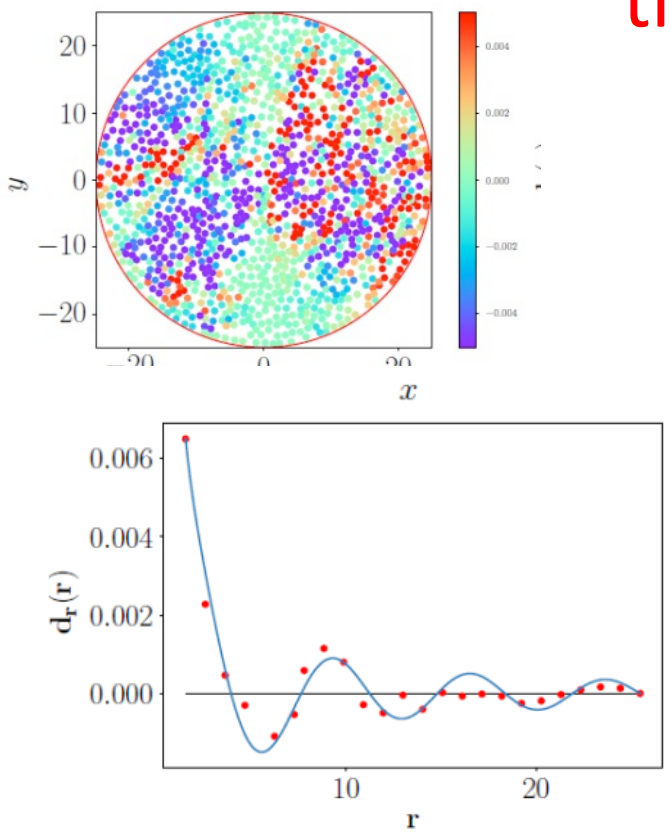

FIG. 5. Radial displacement field with 10% inflation, $\phi = 0.647$. Panel a: Radial displacement field in a planar cross section of the three-dimensional sphere at $z = 0$. One can see the qualitative difference from the map of Fig. 3, with activity going all the way to the outer boundary and displacement pointing inward at places. Panel b: Comparison of the spherical averaged displacement field with $K_n = 2000$ to the theory Eq. (30), using $\kappa = 0.887$. Here $r_{\text{in}} = 1.56$ and $r_{\text{out}} = 24.94$, with $d_0 = 0.0065$.

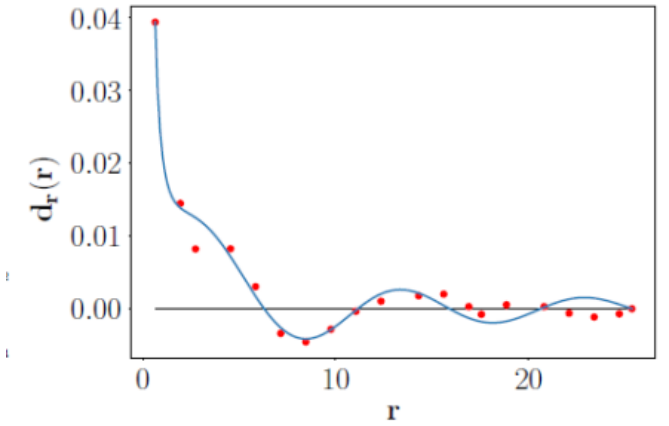

FIG. 6. Radial displacement field with 30% inflation, $\phi = 0.649$. Panel a: Radial displacement field in a planar cross section of the three-dimensional sphere at $z = 0$. Panel b: Comparison of the spherical averaged displacement field with $K_n = 2000$ to the theory Eq. (30), using $\kappa = 0.669$. Here $r_{\text{in}} = 0.65$ and $r_{\text{out}} = 25.35$, with $d_0 = 0.0394$ and $d_r(r_{\text{out}}) = 0$.

Is the transition sharp?

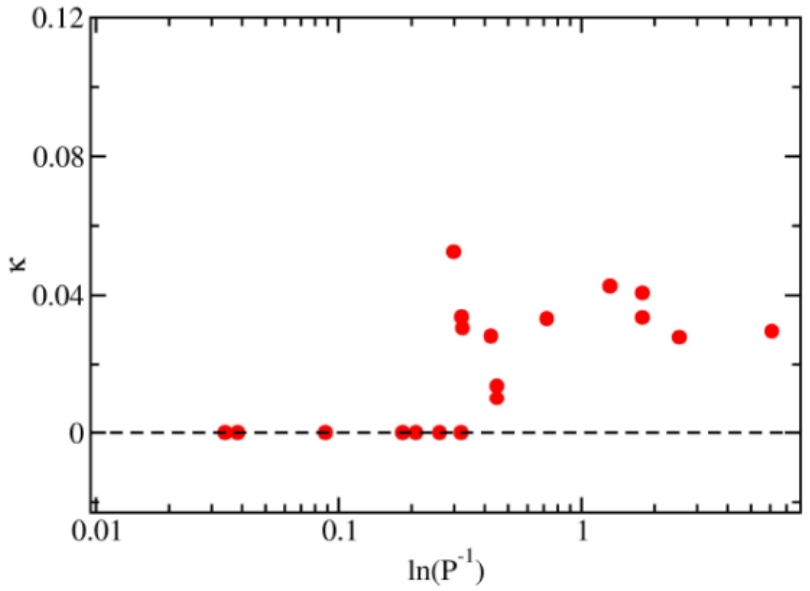

FIG. 3. The screening parameter κ as a function of the logarithm of the inverse pressure. A transition between material phases with quasi-elastic response and with anomalous response is clearly observed.

Explanation

We need an avalanche creating quadrupolar field of size κ^{-1}.

$$Z\ell^{d-1} = \Delta Z \ell^d \ . \qquad p \sim (\phi - \phi_J)^{3/2} \sim \Delta Z^3 \ ,$$

$$\ell \sim \frac{Z}{\Delta Z} \sim p^{-1/3} \ .$$

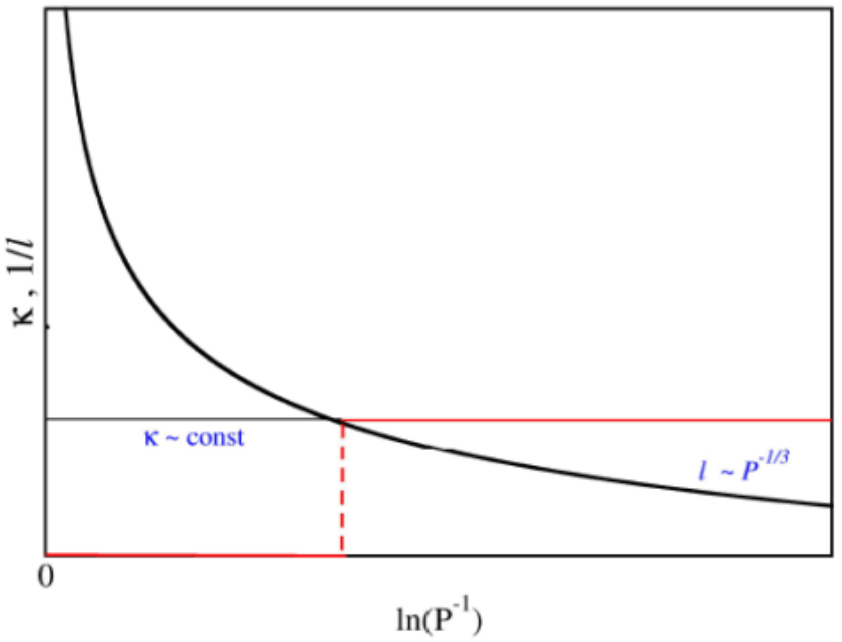

Conclusions and open questions

Plastic events act as screening sources. One can encounter both quadrupolar and dipolar screening.

At least in 2-dimension the transition appears sharp

If correct, then doing theory without taking this into account is like doing electrostatics without knowing about Debye.

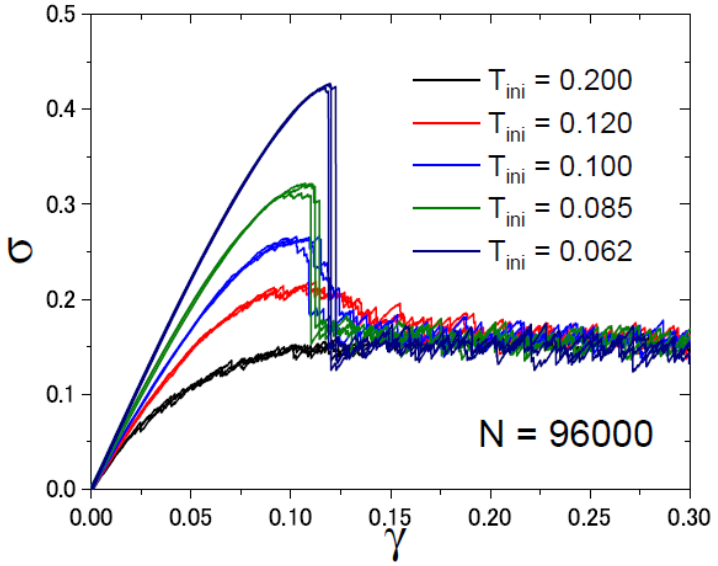

How to explain this? we need to go nonlinear!

Nonlinear dipolar screening?

Dynamics!

Etc. etc.

Thank you very much for your attention!

Colleagues asked: where are the dipoles?

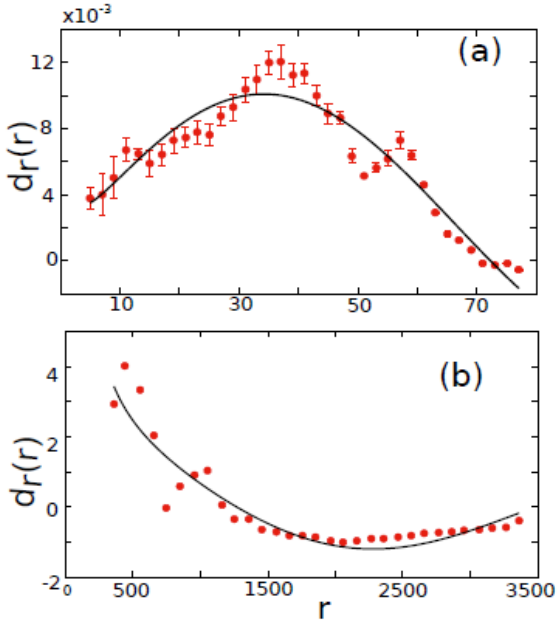

FIG. 1. Angle averaged radial components of the displacement field as measured in simulation and experiment, cf. Refs. [8, 13]. Panel (a): simulations with frictionless Hertzian disks, exhibiting an anomalous response. The continuous line is the solution Eq. (4) with $r_{\rm in} = 4.8$, $r_{\rm out} = 72.2$ and $\kappa = 0.0525$. Panel (b): experimental measurements with frictional disks, The continuous line is the solution Eq. (4) with $r_{\rm in} = 133.3$, $r_{\rm out} = 3478$ and $\kappa = 0.00147$.

$$\frac{1}{Y}\Delta\Delta\chi = \nabla\cdot\mathbf{P} \qquad \frac{1}{Y}\int_\Omega \Delta\Delta\chi \mathrm{dS} = \frac{1}{Y}\oint_{\partial\Omega}(\nabla\Delta\chi)\cdot\mathbf{n}\mathrm{dl} = \frac{1}{Y}\oint_{\partial\Omega}(\nabla p)\cdot\mathbf{n}\,\mathrm{dl}$$

$$\frac{1}{Y}\oint_{\partial\Omega}(\nabla p)\cdot\mathbf{n}\,\mathrm{dl} = \oint_{\partial\Omega}\mathbf{P}\cdot\mathbf{n}\,\mathrm{dl}\,. \qquad p = Y\,\mathrm{Tr}(u),$$

$$\oint_{\partial\Omega}\mathbf{P}\cdot\mathbf{n}\,\mathrm{dl} = \oint_{\partial\Omega}(\nabla(\nabla\cdot\mathrm{d}))\cdot\mathbf{n}\,\mathrm{dl} \equiv I_1\,.$$

$$\nabla\mathrm{Tr}(u) = (\nabla(\nabla\cdot\mathrm{d})) = -\kappa^2\mathbf{d}$$

$$\oint_{\partial\Omega}\mathbf{P}\cdot\mathbf{n}\,\mathrm{dl} = -\kappa^2\oint_{\partial\Omega}\mathbf{d}\cdot\mathbf{n}\,\mathrm{dl}\,.$$

$$I_2 \equiv -\oint_{\partial\Omega}\mathbf{d}\cdot\mathbf{n}\,\mathrm{dl}\,.$$

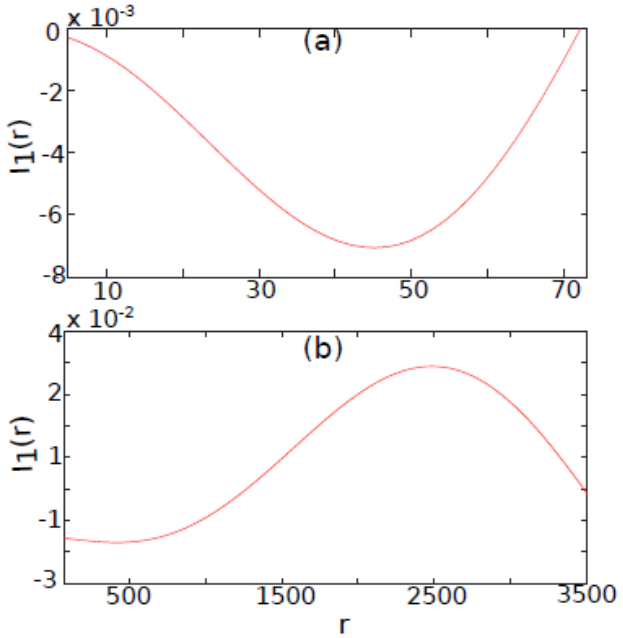

FIG. 2. The integral I_1 of Eq. (10) computed for the two anomalous examples shown in panels (b) and (c) of Fig. 1. The existence of these integrals are a direct demonstration for the presence of dipole fields.

In amorphous solids the response to strain results in plastic events

D. L. Malandro and D. J. Lacks, J. Chem. Phys ,4593 (1999).
C. E. Maloney and A. Lemaitre, Phys. Rev. E 74, 016118 (2006).

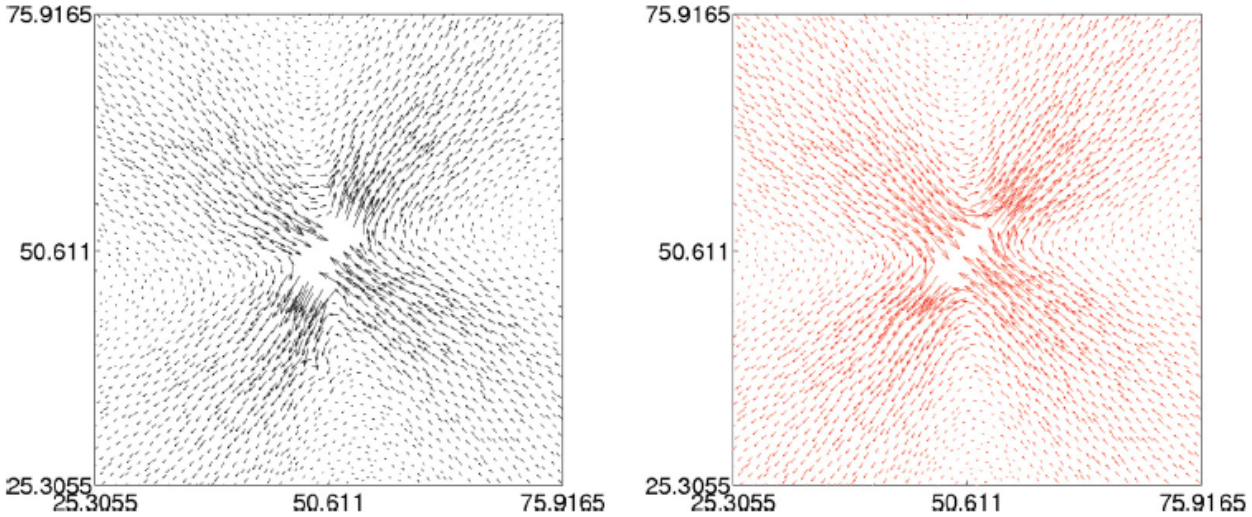

FIG. 1. (Color online) (Left panel) The localization of the nonaffine displacement onto a quadrupolar structure which is modeled by an Eshelby inclusion; see right panel. (Right panel) The displacement field associated with a single Eshelby circular inclusion of radius a; see text. The best fit parameters are $a \approx 3.4$ and $\epsilon^* \approx 0.09$, with a Poisson ratio of $\nu = 0.363$. To remove the effect of boundary conditions, the best fit is generated on a smaller box of size $(x,y) \in [25.30,75.92]$.

Lesson: in elasticity theory monopoles and dipoles cannot be created locally; they are excluded by topology

What about (the beloved) simple shear?

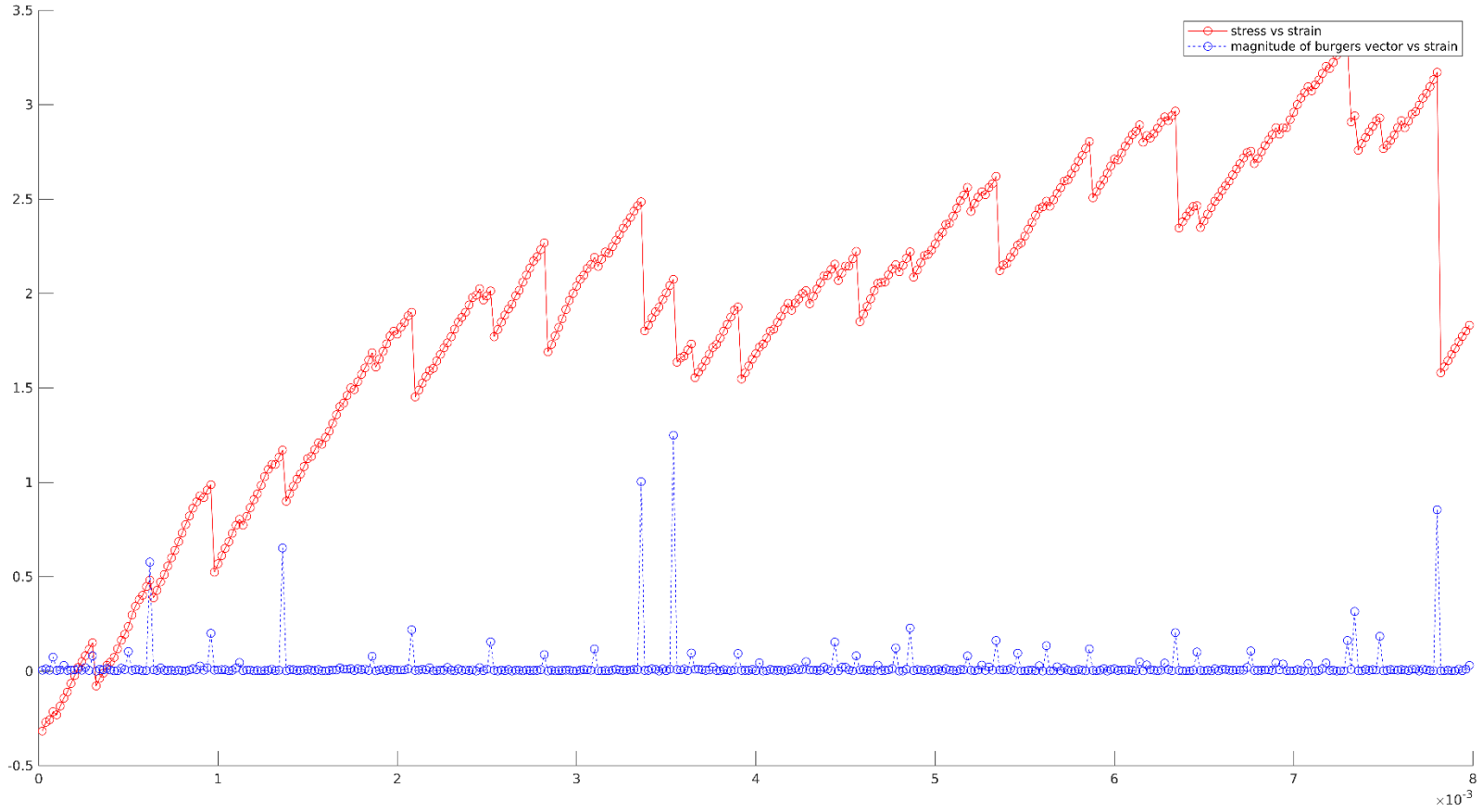

See also: M. Baggioli, I. Kriuchevskyi, Ti. W. Sirk , and A. Zaccone, PRL 127, 015501 (2021)

In the thermodynamic limit any infinitesimal strain results in plastic responses

S. Karmakar, E. Lerner, and I. Procaccia, Phys. Rev. E 82, 055103 (2010).

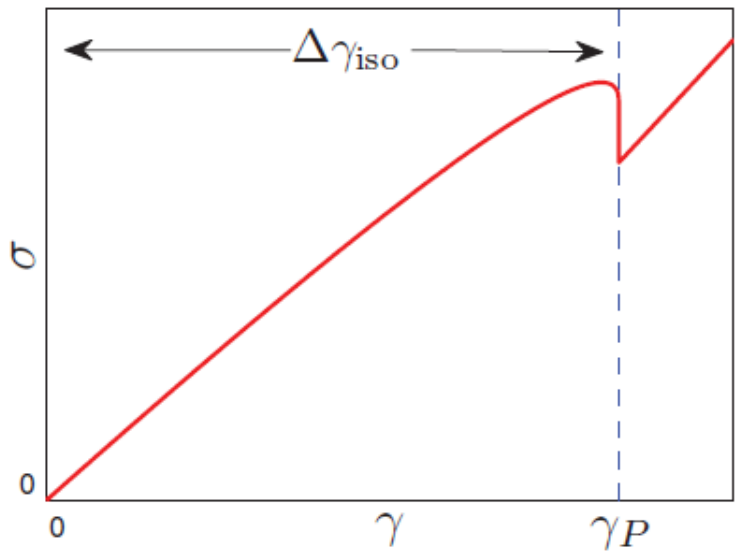

FIG. 2. (Color online) Cartoon of a typical stress vs strain curve of a single instance of the numerical experiment performed in Ref. [6]. Each undeformed system was strained until the first mechanical instability was encountered at some strain value γ_P. Statistics of $\Delta\gamma_{\rm iso} \equiv \gamma_p$ were collected for a variety of system sizes, in both two and three dimensions.

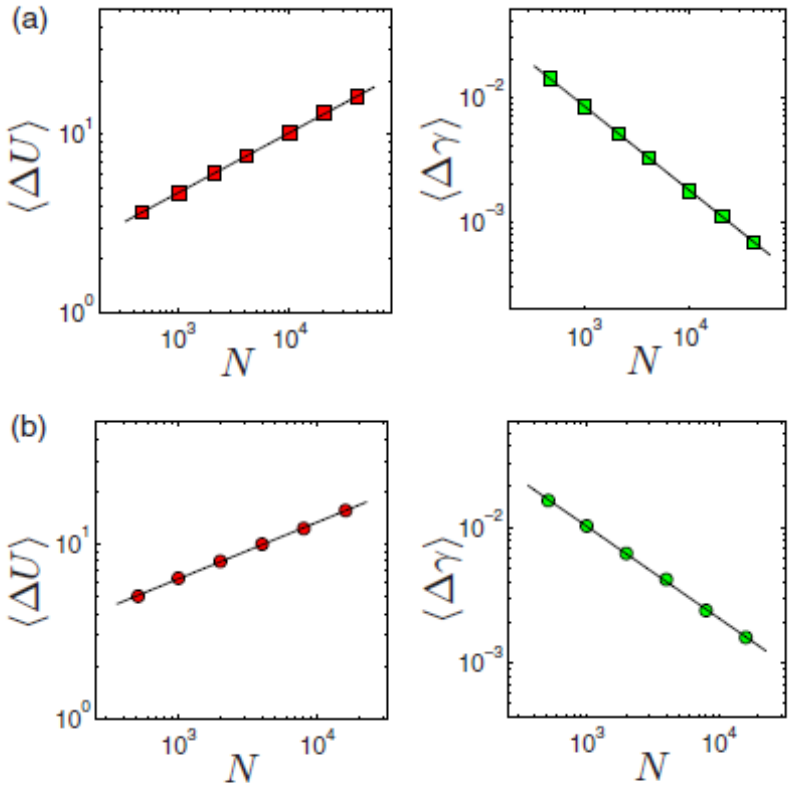

FIG. 2. (Color online) Panel (a). Mean energy drop $\langle\Delta U\rangle$ and mean strain interval $\langle\Delta\gamma\rangle$ in two dimensions as functions of system size, measured in AQS simulations of steady plastic flow of a model glass former, see text. Panel(b). The same for three dimensions. The continuous lines represent the scaling laws (1). The scaling exponents are the same in 2D and 3D.

$$\Delta\gamma_{\rm iso} \sim N^{\beta_{\rm iso}}, \quad \beta_{\rm iso} \approx -0.62.$$

$$\rho\ddot{\boldsymbol{d}} = \frac{Y}{2(1+\nu)}\nabla^2\mathbf{d} + \frac{Y}{2(1+\nu)(1-2\nu)}\nabla(\nabla\cdot\mathbf{d}) + \kappa^2\mathbf{d}\,.$$

$$d_r(r,t) = f_0(r) + f_\omega(r)\cos(\phi+\omega t)\,,$$

$$f_0(r) = d_0\frac{Y_1(r/\lambda_1)J_1(r_{\text{out}}/\lambda_1) - J_1(r/\lambda_1)Y_1(r_{\text{out}}/\lambda_1)}{Y_1(r_{\text{in}}/\lambda_1)J_1(r_{out}/\lambda_1) - J_1(r_{\text{in}}/\lambda_1)Y_1(r_{\text{out}}/\lambda_1)}\,,$$
$$f_\omega(r) = \delta\frac{Y_1(r/\lambda_2)J_1(r_{\text{out}}/\lambda_2) - J_1(r/\lambda_2)Y_1(r_{\text{out}}/\lambda_2)}{Y_1(r_{\text{in}}/\lambda_2)J_1(r_{\text{out}}/\lambda_2) - J_1(r_{\text{in}}/\lambda_2)Y_1(r_{\text{out}}/\lambda_2)} \quad (30)$$

with

$$\lambda_1 = \frac{\mu}{\kappa_1^2}\,, \quad \lambda_2 = \frac{\mu}{\kappa_2^2+\rho\omega^2}\,, \quad \mu = \frac{Y}{1-\nu^2}\,. \qquad (31)$$

In light of this, are amorphous solids really solid??

H. G. E. Hentschel, S. Karmakar, E. Lerner, and I. Procaccia, Do athermal amorphous solids exist?, Phys. Rev.E 83, 061101 (2011).

$$\sigma(\gamma) = \mu(\gamma-\gamma_0)+\frac{1}{2}B_2(\gamma-\gamma_0)^2+\frac{1}{6}B_3(\gamma-\gamma_0)^3+\cdots.$$

To answer this question one needs to examine the sample-to-sample fluctuations of the linear and higher order moduli.

HENTSCHEL, KARMAKAR, LERNER, AND PROCACCIA

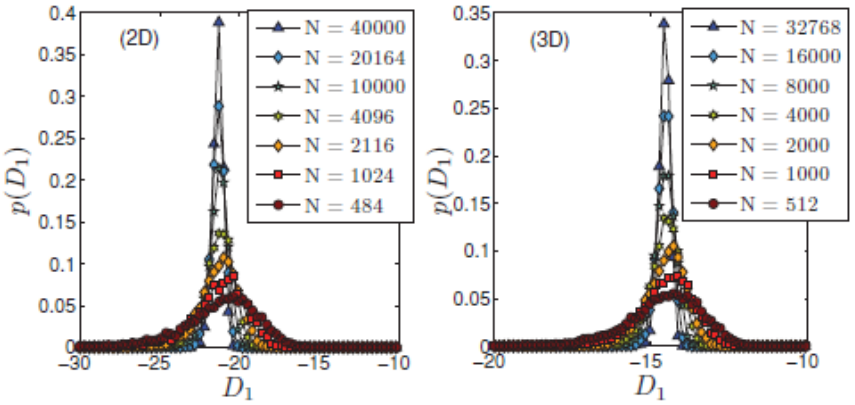

FIG. 6. (Color online) Distributions of D_1 measured for each instance in our ensemble of quenched amorphous solids. As expected, the width of these distributions decays with increasing system size.

Higher order moduli have divergent sample-to-sample fluctuations!

What about dynamics?

$$\mathcal{L} = \frac{\rho}{2} g^{\mu\nu} \dot{d}_\mu \dot{d}_\nu - \frac{1}{2} \sigma^{\mu\nu} u_{\mu\nu} - \frac{1}{2} \Lambda_{\alpha\beta} P^\alpha P^\beta - \Gamma^\alpha_\beta d_\alpha P^\beta$$

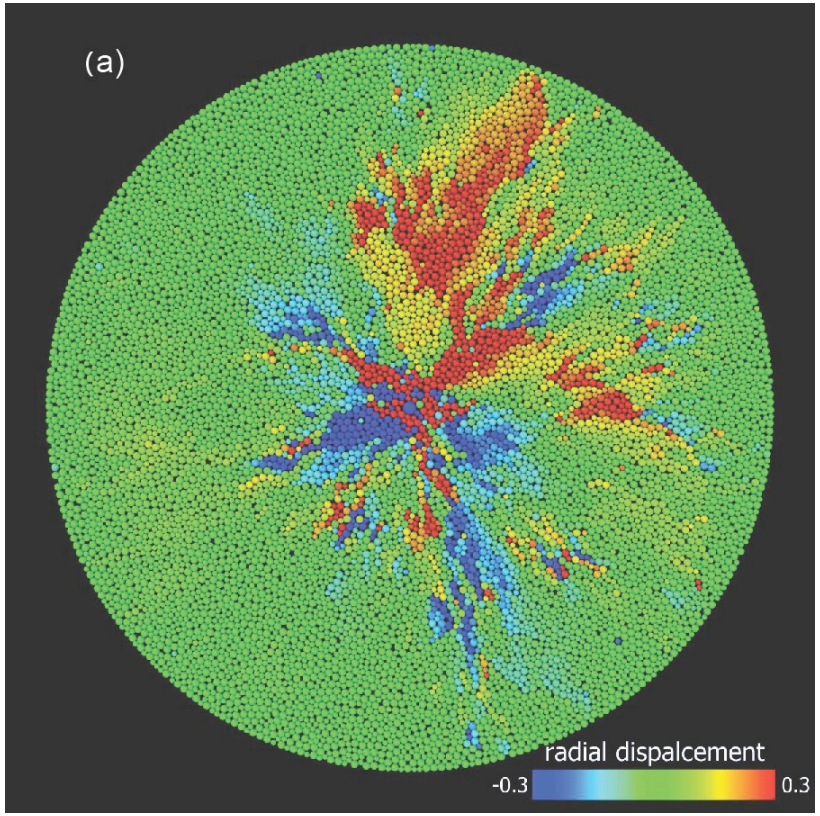

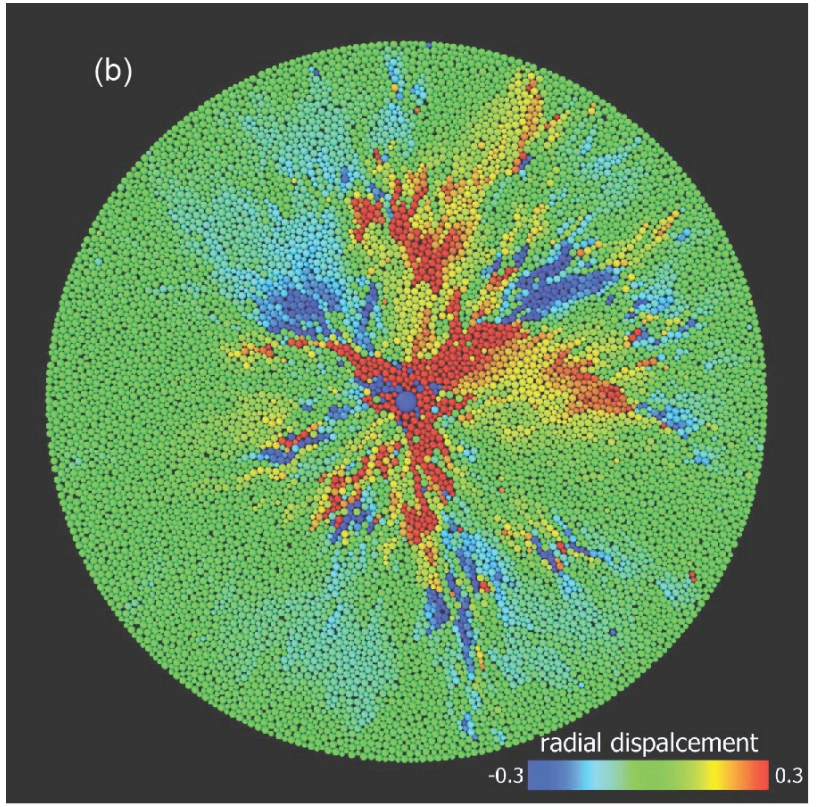

In this lecture I will explain that plastic responses result in screening, dressing elasticity theory in important ways

Reminders from electrostatics: charges (monopoles) and dielectrics (dipoles)

In elasticity theory monopoles and dipoles are topologically protected, plastic events are quadrupolar

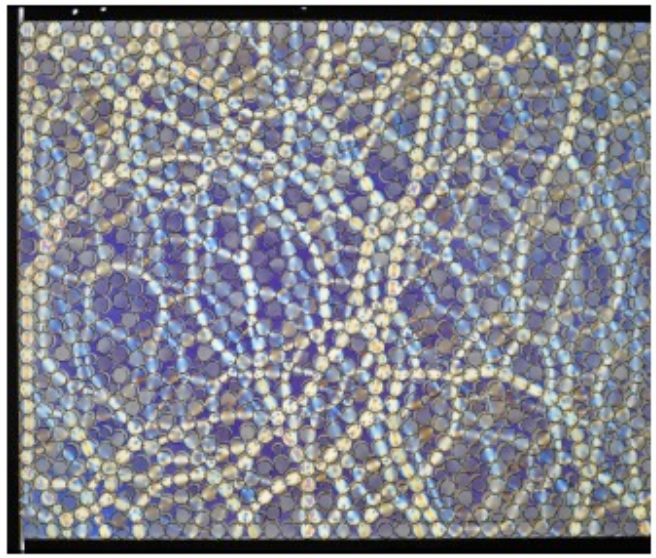

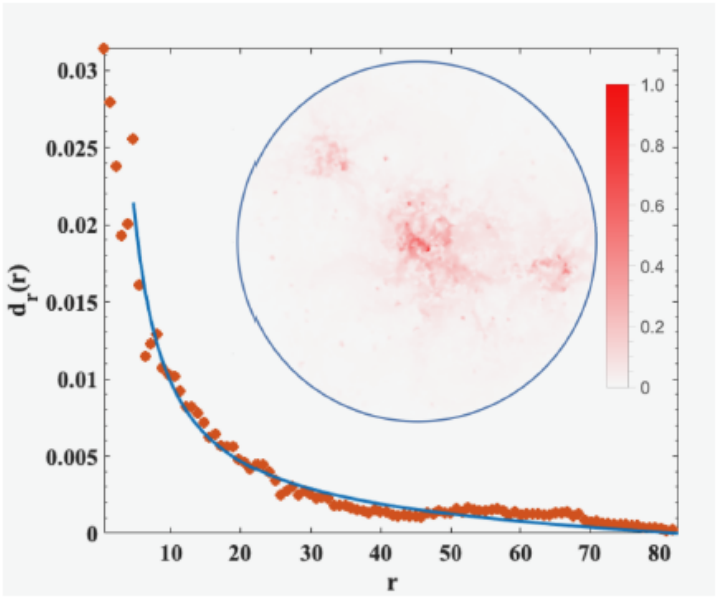

Upon minimizing the energy

$$\partial_\alpha \sigma^{\alpha\beta} = 0$$
$$\sigma^{\alpha\beta} n_\beta|_\partial = t^\alpha \ .$$

$$\Delta \mathbf{d} + \lambda \nabla (\nabla \cdot \mathbf{d}) = 0 \ , \quad \lambda \equiv \frac{1+\nu}{1-\nu}$$

In radial geometry

$$\mathbf{d}(r) = d_r(r)\hat{r},$$

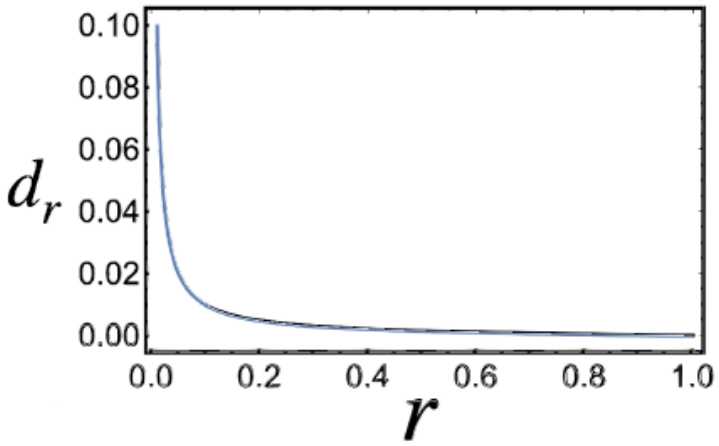

FIG. 3. Graphic representation of the solution of Eq. (9) for $r_{\rm in} = 0.01$ and $r_{\rm out} = 1$, with $d_r(r_{\rm in}) = 0.1$ and $d_r(r_{\rm out}) = 0$.

In purely elastic system

$$F = \int \mathcal{L}\, \mathrm{d}^2x - \oint t^\beta d_\beta \, \mathrm{d}l \ ,$$
$$\mathcal{L} = \frac{1}{2} A^{\alpha\beta\gamma\delta} u_{\alpha\beta} u_{\gamma\delta} = \frac{1}{2} \sigma^{\alpha\beta} u_{\alpha\beta} \ . \qquad (1)$$

The strain is related with the displacement field via

$$u_{\alpha\beta} = \frac{1}{2} \left(\partial_\alpha d_\beta + \partial_\beta d_\alpha \right) \ . \qquad (2)$$

The surprise

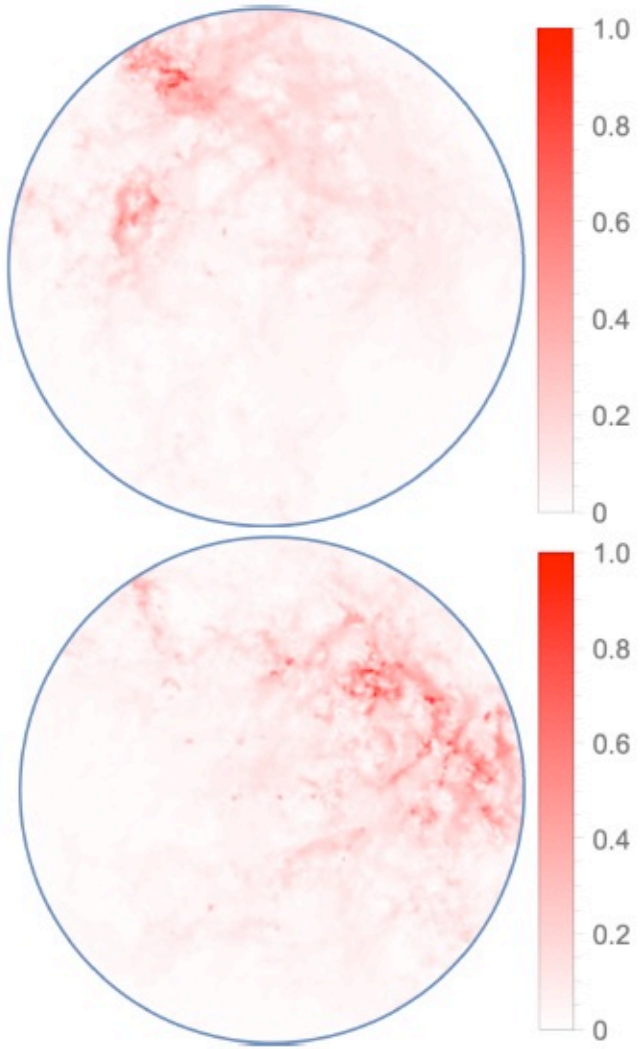

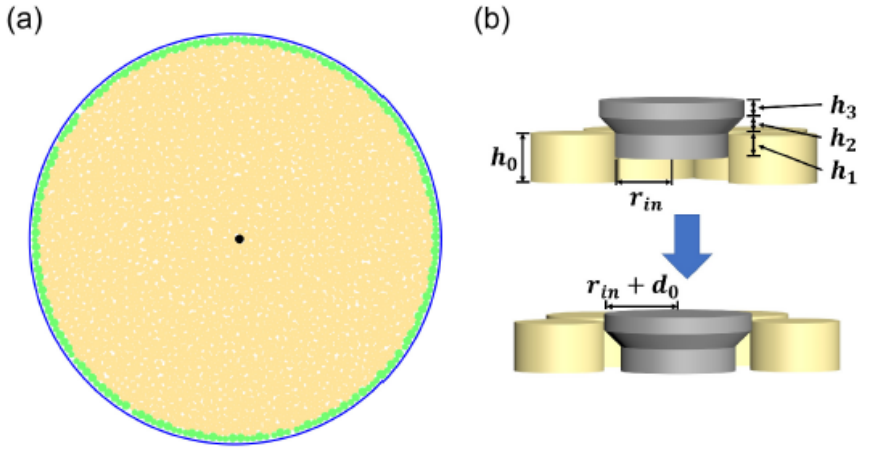

FIG. 1. Panel (a): Top view of the experimental system. The blue line marks the position of the circular boundary. The green layer represent the photo-elastic disks at the circumference, which are used as pressure sensors. In the yellow area, either the bi-disperse ABS disks or the bi-disperse photo-elastic disks are filled in, see text for details. The black dot in the center represents the conical shaped pusher used to achieve the inflation. Panel (b) A diagram of the inflation process. Here $r_{in} = 7.0$ mm, $d_0 = 0.7$ mm, $h1 = 2.0$ mm, $h2 = 0.7$ mm, and $h_3 = 3.0$ mm for the conical shaped pusher in the low dimensionless pressure experiment, and $r_{in} = 14.0$ mm, $d_0 = 1.4$ mm, $h1 = 2.0$ mm, $h2 = 1.4$ mm, and $h_3 = 3.0$ mm in the high dimensionless pressure experiment. The value of h_0 depends on the pusher type: $h_0 = 8.0$ mm for the ABS disks, and $h_0 = 6.0$ mm for the photo-elastic disks.

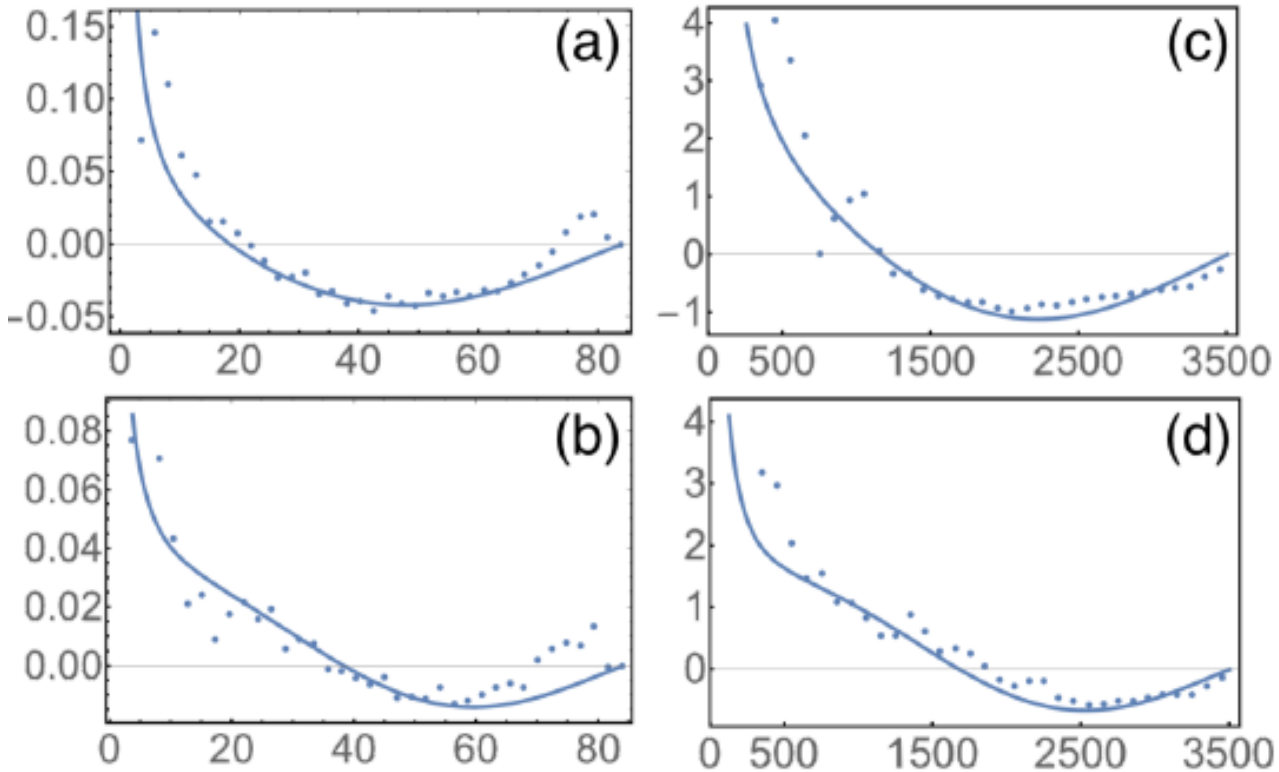

FIG. 3. Radial component of the Displacement field induced by the inflation of one disk at the center of the box. Panel (a) and (b): simulation results at pressure $\tilde{P} = 2 \times 10^{-7}$, $\phi \approx 0.845$ with inflation of 80%. $r_{\text{in}} = 1.14$ and $r_{\text{out}} = 83.82$, $\kappa = 0.0525$ and 0.0706 in panels (a) and (b) respectively. Panels (c) and (d): experimental results at pressure $\tilde{P} \approx 10^{-6}$ and inflation of 10%, $r_{\text{in}} = 70$ and $r_{\text{out}} = 3500$, $d_0 = 7$. Here $\kappa = 0.0014$ and 0.00176 in panels (c) and (d) respectively.

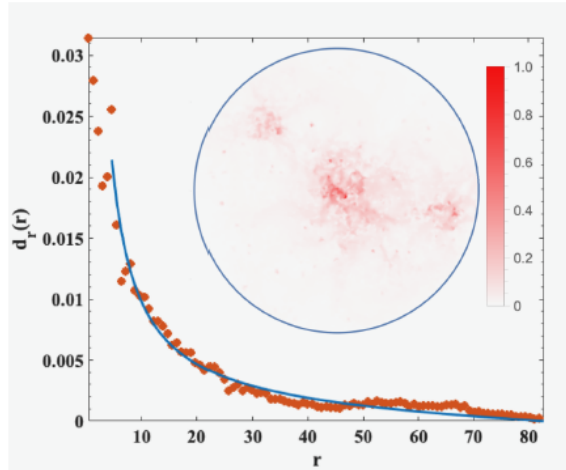

FIG. 4. Displacement field for $P = 40$. Inset: the displacement field caused by inflating one disk closest to the origin by 1%. Here the displacement vectors are normalized and color coded as in Fig. 1. Shown also is the fit of Eq. (9) to the angle-averaged displacement. Here the parameters used in the fit are $d_0 = 0.03028$; $r_{\text{in}} = 3.268$; $r_{\text{out}} = 82.74$.

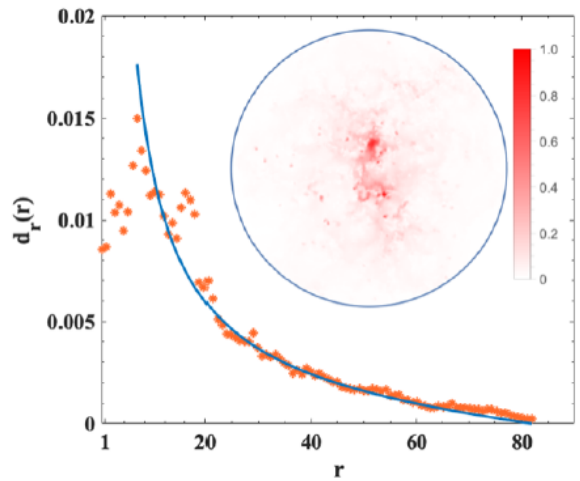

FIG. 5. Displacement field for $P = 60$. Inset: the displacement field caused by inflating one disk closest to the origin by 1%. The displacement vectors are normalized and color coded as in Fig. 1 Shown also is the fit of Eq. (9) to the angle-averaged displacement. Here the parameters used in the fit are $d_0 = 0.03487$; $r_{\text{in}} = 3.631$;$r_{\text{out}} = 81.9$.

The analogy to the hexatic phase in 2-dimensional melting

In an ideal hexagonal crystal, each particle touches six others.

As the crystal melts, this order begins to fall apart. Some particles gain a neighbor and others lose one, although the large-scale order of the material remains unchanged. The elastic moduli though soften, analogously to our dilute quadrupole density.

When pairs of 5-7 neighbors form stably, we enter the hexatic phase. These are dipoles! Now the translational order disappears, but orientational order remains

Finally 5 and 7 coordinated particles dissociate, and these are monopoles, heralding the liquid phase.

Experimental verification (Jin Shang and Jie Zhang)

arXiv:2108.13334

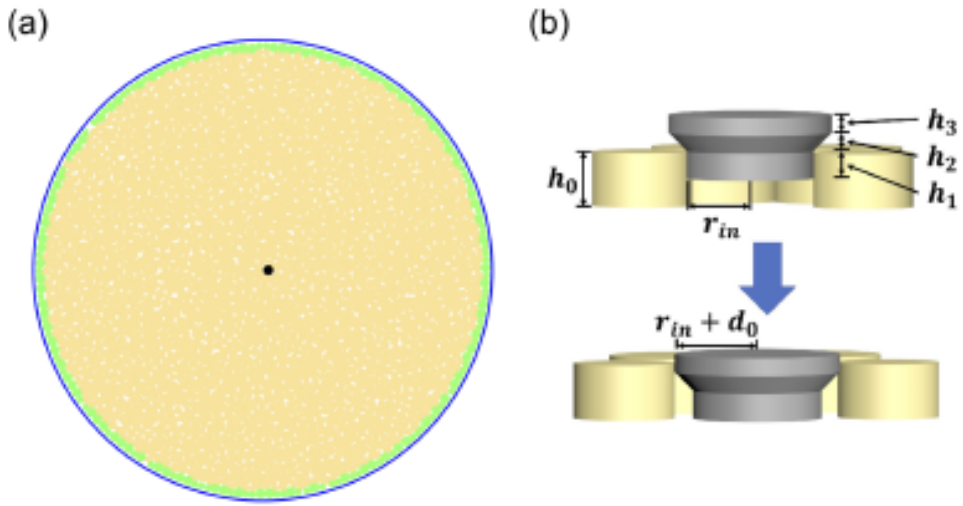

They use disks of acrylonitrile butadiene styrene (ABS) of two different radii (7 and 5.5 mm), with a number ratio 1:1. The outer circular frame is shown as a blue layer, with an inner layer of photo-elastic disks (green layer) that act as pressure sensors. Inflation is achieved with the (grey) conical pusher.

After inflation the displacement field is measured and the radial component is computed

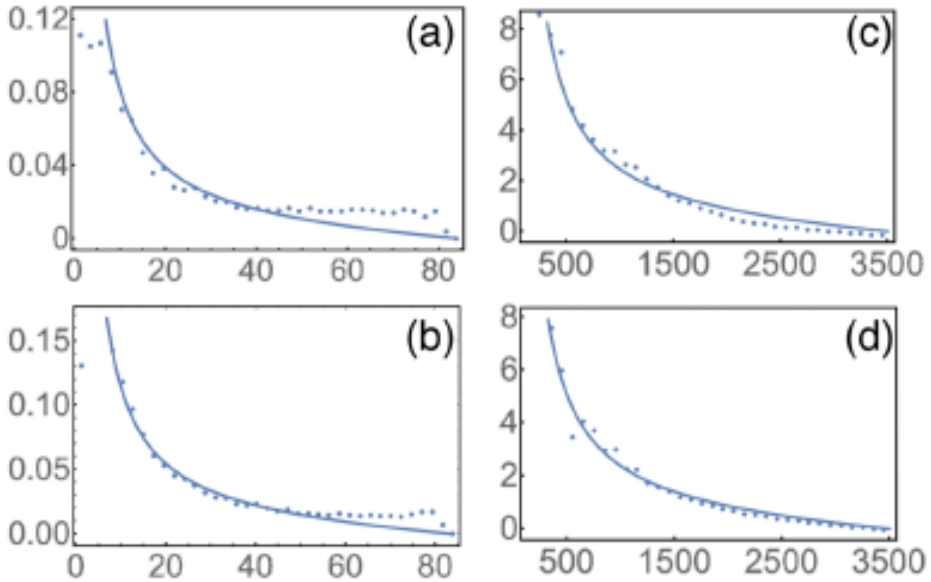

FIG. 2. Radial component of the Displacement field induced by the inflation of one disk at the center of the box. Panels (a) and (b) simulation results at dimensionless pressure $\tilde{P} = 2.25 \times 10^{-6}$, $\phi \approx 0.872$ with inflation of 10%. Here $r_{\text{in}} = 1.14$ and $r_{\text{out}} = 83.82$. $d_0 = 0.7$ and 1 in panels (a) and (b) respectively. Panels (c) and (d): experimental results at pressure $\tilde{P} \approx 10^{-3}$ with inflation of 10%. Here $r_{\text{in}} = 140$ and $r_{\text{out}} = 3500$, $d_0 = 19.1$ and 18.3 respectively.

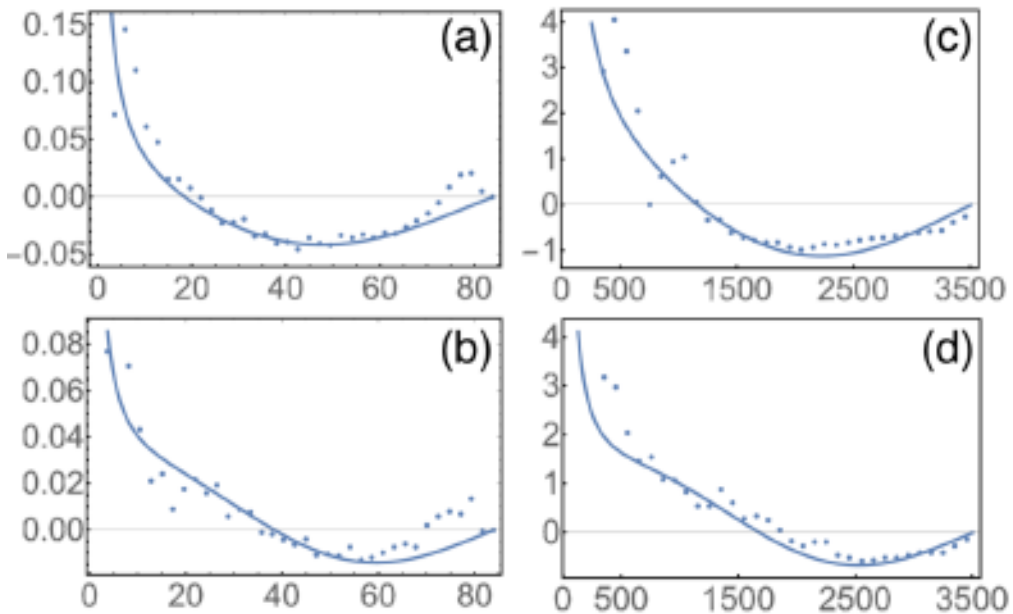

FIG. 3. Radial component of the Displacement field induced by the inflation of one disk at the center of the box. Panel (a) and (b): simulation results at pressure $\tilde{P} = 2 \times 10^{-7}$, $\phi \approx 0.845$ with inflation of 80%. $r_{\text{in}} = 1.14$ and $r_{\text{out}} = 83.82$, $\kappa = 0.0525$ and 0.0706 in panels (a) and (b) respectively. Panels (c) and (d): experimental results at pressure $\tilde{P} \approx 10^{-6}$ and inflation of 10%, $r_{\text{in}} = 70$ and $r_{\text{out}} = 3500$, $d_0 = 7$. Here $\kappa = 0.0014$ and 0.00176 in panels (c) and (d) respectively.

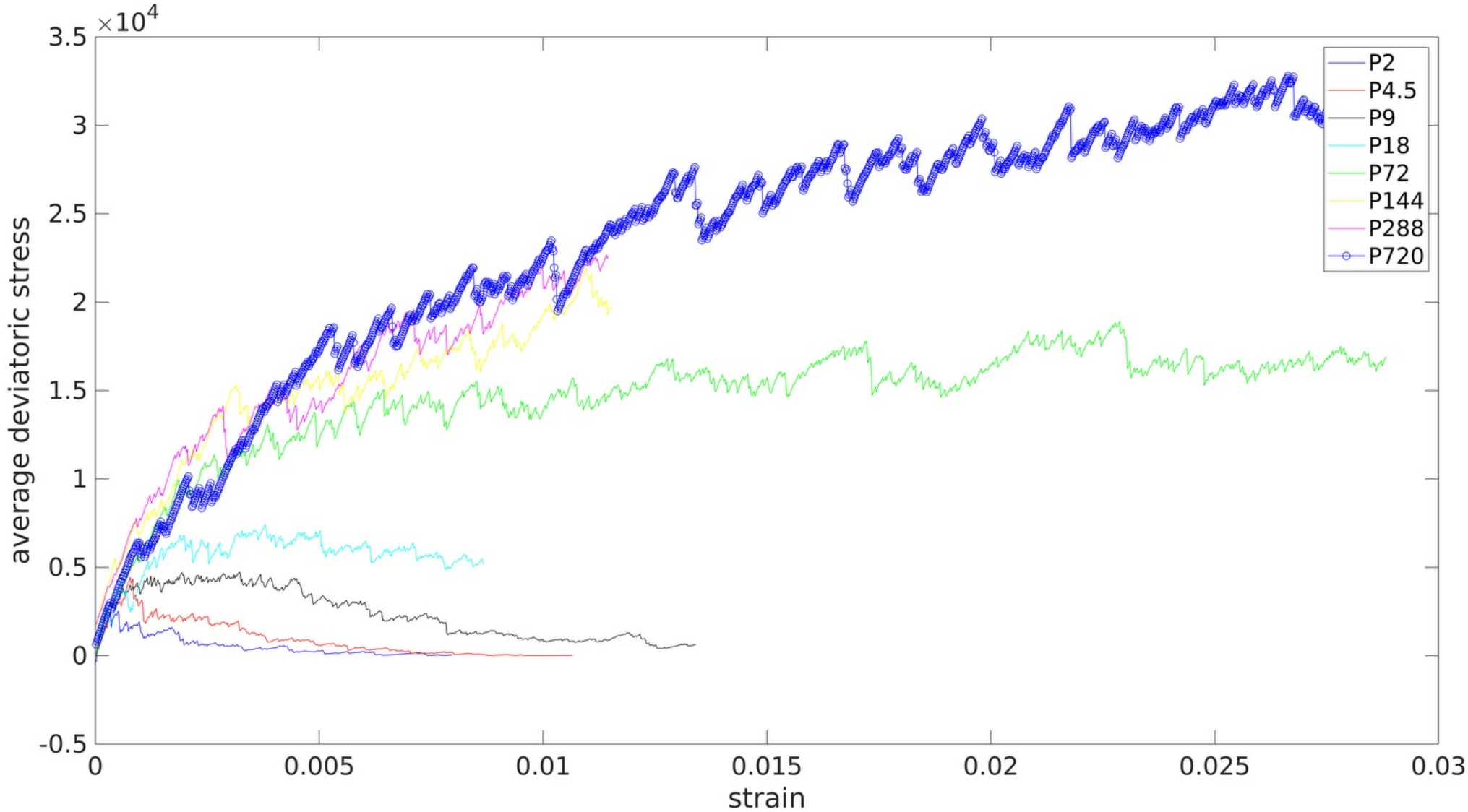
×10^4
3.5
3
2.5
2
1.5
1
0.5
0
-0.5
average deviatoric stress
0
0.005
0.01
0.015
0.02
0.025
0.03
strain
P2
P4.5
P9
P18
P72
P144
P288
P720

Challenges

1. Show that there exists a phase transition (we work at T=0, so what is the natural parameter?)

2. Examine classical models of glass formers (with point particles). (We know that fast quench to T=0 results in extensive plasticity upon strain, and slow quench in much less plastic response).

3. What is happening in three dimensions?

4. Examine richer protocols of strain (space dependent inflation, space dependent shear?)

5. Do we need to rewrite elasticity theory for amorphous materials?

Another example

$$\Delta \mathbf{d} + \lambda \nabla (\nabla \cdot \mathbf{d}) = -\mu \mathbf{d}$$

μ=7

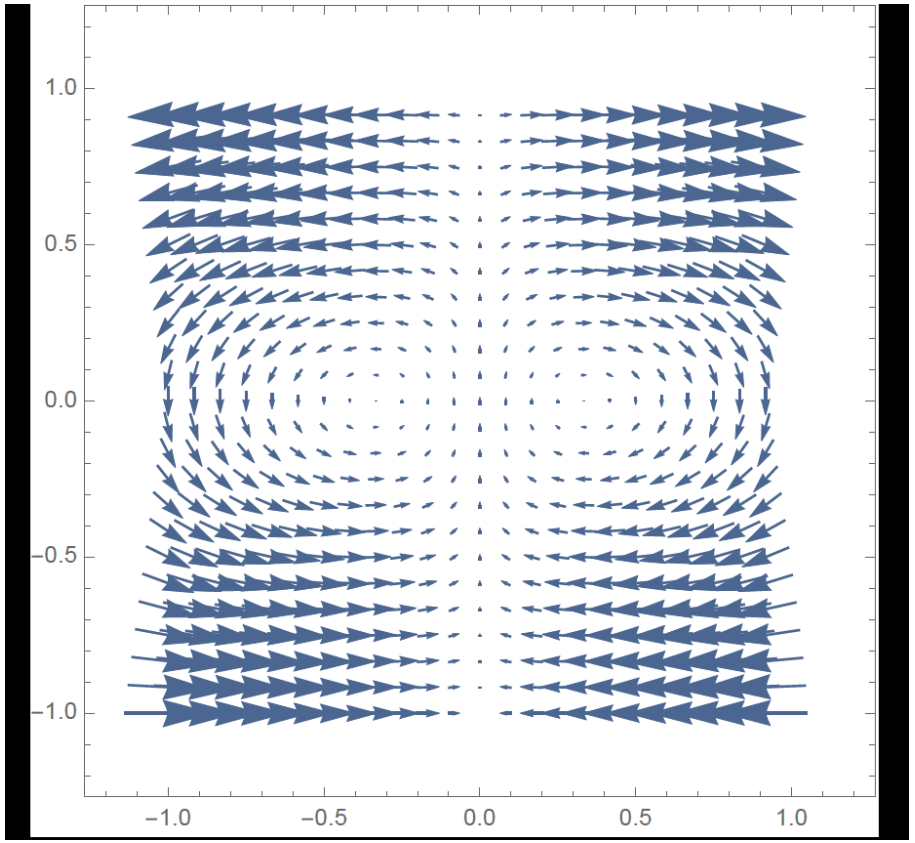

μ=0

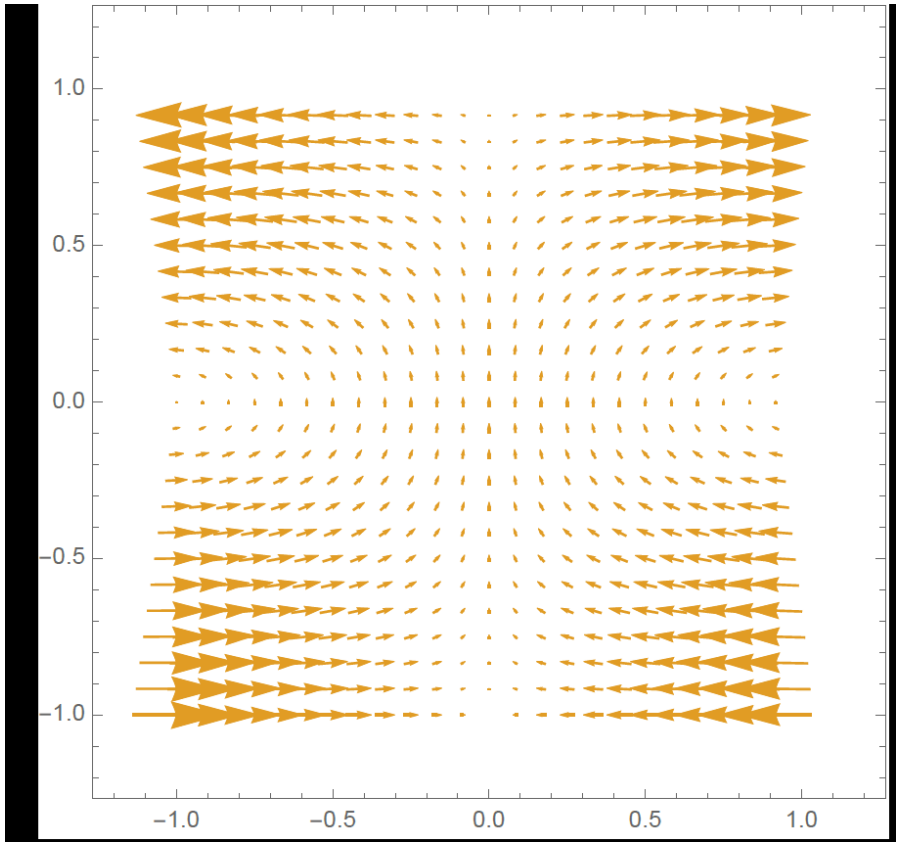

The y component of the displacement along x=1,-1<y<1